Self-Assembly

DOI: 10.1002/anie.201403572

Surface-Confined Self-Assembled Janus Tectons: A Versatile Platform towards the Noncovalent Functionalization of Graphene**

Ping Du, Maud Jaouen, Amandine Bocheux, Cyril Bourgogne, Zheng Han, Vincent Bouchiat, David Kreher, Fabrice Mathevet, Céline Fiorini-Debuisschert, Fabrice Charra, and André-Jean Attias**

Abstract: *A general strategy for simultaneously generating surface-based supramolecular architectures on flat sp^2-hybridized carbon supports and independently exposing on demand off-plane functionality with controlled lateral order is highly desirable for the noncovalent functionalization of graphene. Here, we address this issue by providing a versatile molecular platform based on a library of new 3D Janus tectons that form surface-confined supramolecular adlayers in which it is possible to simultaneously steer the 2D self-assembly on flat $C(sp^2)$-based substrates and tailor the external interface above the substrate by exposure to a wide variety of small terminal chemical groups and functional moieties. This approach is validated throughout by scanning tunneling microscopy (STM) at the liquid–solid interface and molecular mechanics modeling studies. The successful self-assembly on graphene, together with the possibility to transfer the graphene monolayer onto various substrates, should considerably extend the application of our functionalization strategy.*

Although adsorbing organic molecules on surfaces is the most used method to modify the properties of the substrate, a strategy for developing complex, well-ordered adlayers with tailored functionalities remains a key issue in nanotechnology. This is why, in addition to covalent functionalization through a strategy based on self-assembled monolayers (SAMs),[1] two-dimensional (2D) supramolecular self-assembly by noncovalent adsorption of planar organic building blocks (tectons) at metal or highly oriented pyrolitic graphite (HOPG) surfaces has attracted considerable interest.[2–6] This approach allows hydrogen bonding, metal–ligand coordination, or alkyl chain interdigitation to be used to generate functional hybrid interfaces of networks that exhibit in-plane functionalities, for example, hosting subsequent deposited species in the case of porous molecular networks.[4,7,8] Recently, a few elegant strategies exploiting the 2D in-plane positioning on various conducting substrates have been developed to achieve the controlled positioning of molecules out-of the plane so as to add a functionality which does not disturb the 2D self-assembly and which is preserved from possibly detrimental influences of the substrate. These routes towards three-dimensional (3D) self-assembled systems consist of the surface-confined self-assembly of 3D tectons,[9] mainly based on cyclophanes,[10] sandwich-type multidecker complexes,[11] or azobenzene-functionalized triazatriangulenium derivatives.[12] However, in the above examples, the functionality drives the building-block design;[13] thus, the 2D organization and the functionalities are often carried by the same constitutive moieties and these strategies suffer from a lack of versatility. On the other hand, besides covalent functionalization, noncovalent functionalization of graphene has received tremendous interest since it offers the possibility of attaching a functionality while maintaining the integrity of the sp^2-hybridized carbon network, that is, without disturbing the electronic properties of the substrate.[14a] This aspect is critical as far as electronic devices are concerned. Indeed, it is known that even a low density of sp^3 grafting strongly affects the delocalization of electrons within the graphene layer, thus making it incompatible for applications such as sensors.[14b] Finally, an adsorbed molecular lattice is able to impose a super-period to the graphene atomic lattice. This is considered to be a new method to finely tune its band and sub-band structure for use as innovative 2D semiconductor junctions.[14c] The most used noncovalent approach consists of binding pyrene-substituted species through π-π interactions without forming a well-ordered adlayer.[15] Recently it was demonstrated, for a few molecules, that the same principles reported above for the molecular in-plane confined self-assembly on substrates such as HOPG can be transferred to graphene. Thus, well-ordered 2D molecular layers self-assembled through hydrogen bonding[16] or other weak interactions can be formed on graphene.[17] However, to

[*] Dr. P. Du, Dr. A. Bocheux, Dr. D. Kreher, Dr. F. Mathevet, Prof. A. J. Attias
Institut Parisien de Chimie Moléculaire, Chimie des Polymères
UMR CNRS 8232, Université Pierre et Marie Curie
3 rue Galilée, 94200 Ivry (France)
E-mail: andre-jean.attias@upmc.fr
Dr. C. Bourgogne
Equipe Architectures Moléculaires et Matériaux Nanostructurés
Institut Charles Gerhardt, UMR CNRS 5253
8 rue de l'Ecole Normale, 34296 Montpellier Cedex 5 (France)
Z. Han, Dr. V. Bouchiat
Department Nanosciences, Institut Neel, CNRS
Univ. Grenoble-Alpes
38042 Grenoble Cedex 09 (France)
M. Jaouen, Dr. C. Fiorini-Debuisschert, Dr. F. Charra
Laboratoire de Nanophotonique
Service de Physique de l'Etat Condensé, CEA/Saclay
91191 Gif sur Yvette Cedex (France)
E-mail: fabrice.charra@cea.fr

[**] We thank the French Research National Agency (ANR) (NOMAD project ANR-08-NAN O-013-02; NANOCRISNET project ANR-11 BS-1001801), Ville de Paris (Research in Paris Program), AOARD (Grant FA2386-12-1-4011), and EU Graphene flagship for financial support.

Supporting information for this article is available on the WWW under http://dx.doi.org/10.1002/anie.201403572.

 © 2014 Wiley-VCH Verlag GmbH & Co. KGaA, Weinheim

date routes towards adding functionality to graphene through surface-confined self-assembly of 3D tectons have remained unexplored. Therefore, a general, versatile, and convenient strategy for simultaneously generating surface-based supramolecular periodic architectures on sp^2-hybridized carbon supports such as HOPG and graphene, and independently exposing on demand off-plane functionalities with controlled lateral order is highly desirable.

We recently proposed the Janus tecton concept,[18] a two-faced 3D building block where one face acted as a pedestal that steered the 2D self-assembly on HOPG through alkyl chain interdigitation, while the other face was a π-conjugated chromophore lifted from the substrate through a pillar linking the two faces. However this approach suffered some drawbacks because of the pillar design and synthetic route, which led to low yields and lack of versatility. Here, to tackle these problems, we completely revisited and rationalized the pillar (**P**) design as well as the synthetic sequence to provide a versatile molecular platform based on a library of new 3D Janus tectons (**JAP** and **JA**; Scheme 1) able to form surface-confined supramolecular adlayers in which it is possible to simultaneously a) steer the 2D self-assembly on flat $C(sp^2)$-based substrates with controlled lateral order to form periodic patterns and b) tailor the external interface above the substrate by exposing a wide variety of small terminal chemical groups (-CN, $-CO_2Me$, -CHO, $-CO_2H$, -Br) and functional moieties for further potential use, for example, for hydrogen bonding, metal–ligand bonding, and redox processes. This approach is validated throughout the self-assembly process by scanning tunneling microscopy (STM) at the liquid–HOPG and liquid–graphene interface and molecular mechanics modeling studies.

When designing the **P** key building blocks (Scheme 1), three basic criteria were taken into account when choosing the skeleton and the exposed functional groups: a) **P** should be prepared using as few steps as possible to later obtain the two kinds of Janus tectons, **JAP** and **JA**, on a large scale; b) **P** should be able to expose various terminal chemical functional groups (R^1) on the upper face so that different classes of organic reactions could be used to ultimately attach a broad range of functional units; c) the chemical group R^1 should be uncompetitive during the synthesis steps to obtain the Janus tecton precursors from **P** compounds, and R^2 should be sufficiently active to generate on demand, through only a "one-step reaction", the functional unit (R^3). To fulfill all these criteria, the dithia[3.3]metaparacyclophane skeleton was chosen and used for the first time for building complex 3D structures. Despite the fact that there are currently few reports on its derivatization,[19] the main interesting feature is the dihedral angle between the *meta*- and *para*-substituted rings (ca. 11–15°).[19c] This very small change should induce drastic effects compared to the paracyclophane unit we previously used. We expect that 1) the reactivity of the functional chemical groups would be better for attaching the functional units (less steric hindrance between the functional group and neighboring CH_2 group in comparison with the dithia[3.3]paracyclophane structure), and 2) the metaparacyclophane architecture should allow us to lift the functional moiety with an outward angle, thereby avoiding direct contact

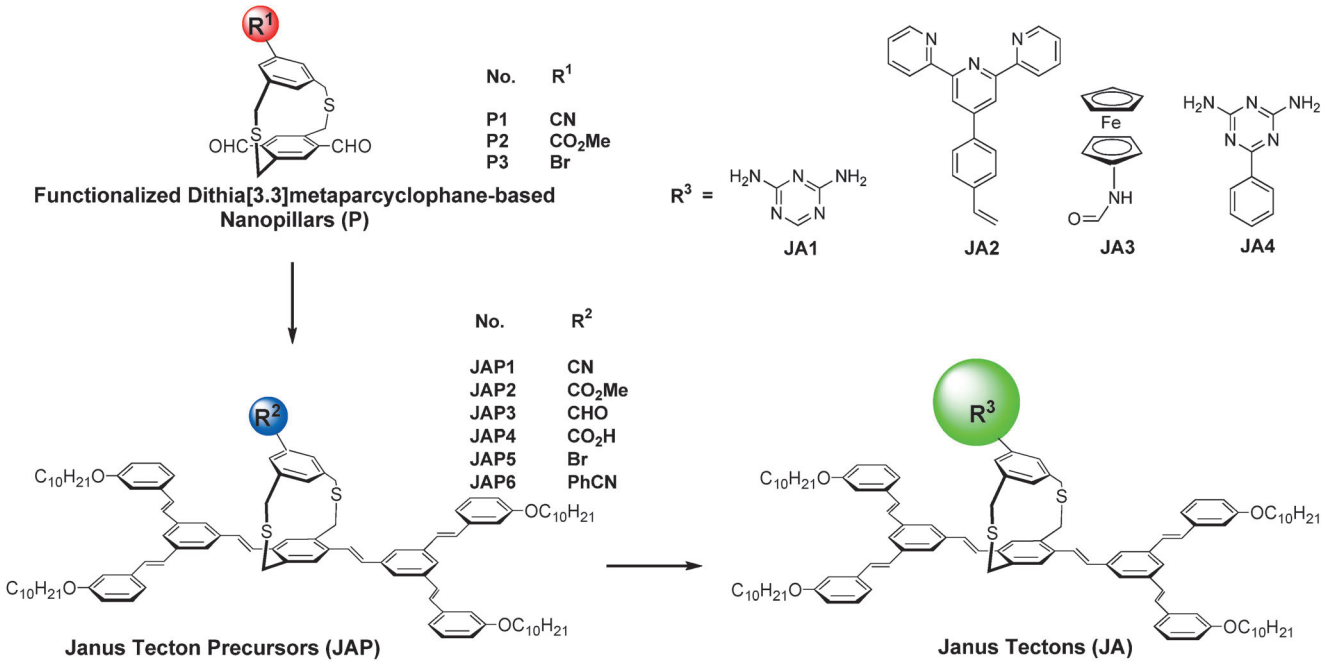

Scheme 1. Synthesis strategy. The lower deck of dithia[3.3]metaparacyclophane-based functionalized nanopillars (**P**) bearing a chemical group on the upper deck (R^1) is end-capped with two molecular clip units to generate Janus tecton precursors (**JAP**), which consists of a pedestal for steering the 2D self-assembly on flat $C(sp^2)$-based supports and a pillar exposing a chemical group (R^2). A post-functionalization leads to Janus tectons (**JA**) presenting a wide range of functionalities (R^3). After adsorption on substrates, the self-assembled Janus tectons should allow the on-demand noncovalent functionalization by control of the functionality of the exposed surface of the adlayer.

 © 2014 Wiley-VCH Verlag GmbH & Co. KGaA, Weinheim

between large functional units (see **JA2** and **JA3**) and the substrate surface.

On the basis of the above considerations, we designed and synthesized, by adapting literature procedures, three functionalized pillars **P** bearing cyano, ester, and bromo groups as chemical functions R^1 on the top ring of the pillar and two aldehyde groups on the bottom ring of the pillar (see Figure S1 in the Supporting Information for experimental details).

The aldehyde groups of the functionalized pillars **P** were then used to build the pedestal of the Janus tecton precursors **JAP1**, **JAP2**, and **JAP5** (Scheme 1). A Horner–Wadsworth–Emmons coupling reaction between the "molecular clip" we had previously designed for surface-specific supramolecular bonding on HOPG[8e] and nanopillars **P1**, **P2**, and **P3** gave **JAP1**, **JAP2**, and **JAP5**, respectively, in one step and in good yield (see Figure S2 in the Supporting Information). These Janus tecton precursors can be considered as the parent structures and used to enlarge the series, one parent nanopillar **P** equipped with a chemical group R^1 being able to generate a **JAP** bearing either the same chemical group ($R^2 = R^1$) or a new chemical group ($R^2 \neq R^1$; see Figure S2 in the Supporting Information). For example, **P1** only generates **JAP1**, with both compounds exposing the same terminal cyano group, whereas **P2** and **P3** give two series of Janus tecton precursors that exhibit various terminal groups, **JAP2**–**JAP4** and **JAP5** and **JAP6**, respectively. In the former series, the subsequent reduction of **JAP2**, which has the same terminal ester group as **P2**, with DIBAL-H followed by oxidation of the intermediate compound with PCC affords Janus tecton precursor **JAP3** in 31 % yield in two steps. **JAP2** can also give Janus tecton precursor **JAP4** through hydrolysis of the CO_2Me ester group. In the other series, **JAP5** exposes the same terminal ester group as **P3**, and a one-pot Suzuki coupling between **JAP5** and 4-cyanophenylboronic acid affords **JAP6** in 61 % yield.

Finally, all the target **JA1**–**JA4** tectons were obtained in one-step from the corresponding **JAP** precursors (see Figure S3 in the Supporting Information). For example, the conversion of the nitrile group of Janus tecton precursor **JAP1** with dicyandiamide into a 2,6-diamino-*s*-triazine hydrogen-bonding unit[20] afforded **JA1** in 28 % yield. The same procedure allowed the conversion of **JAP6** into **JA4** in 26 % yield. Building block **JA2** was obtained in 88 % yield by the Horner–Wadsworth–Emmons reaction between **JAP3** and phosphonate-functionalized terpyridine with an excess of base under reflux in toluene.[21] Tecton **JA3** was prepared through the condensation of compound **JAP4** with aminoferrocene, in 39 % yield. All the **JA** tectons were characterized by ^1H and ^{13}C NMR spectroscopy as well as low-resolution MALDI-TOF and high-resolution ESI mass spectroscopy.

The self-assembly properties of the Janus tecton precursors (**JAP**) and Janus tectons (**JA**) were investigated first by STM at the liquid–HOPG interface at room temperature (for experimental details, see the Supporting Information). Typical STM images of **JAP4** and **JA1-4** are reported in Figure 1. Since they have been acquired at high bias ($|V_T| \geq 1200$ mV) the bright spots are attributable to the upper level (functional moiety) of the Janus tectons that form a periodic lattice, which shows that all the probed 3D tectons spontaneously self-assemble into 2D networks on HOPG. The lattice parameters of each network could be measured after a careful correction of the thermal drift, based on a cross-correlation between two successive images. It turns out that irrespective of the building block, the lattice parameters are all the same within the typical experimental accuracy of ± 5 % for the distances and $\pm 2°$ for the angles and are compatible with those of the lattice formed by the ground floor (**GF**)[8e] which acts as pedestal in the **JAP** and **JA** tectons (see Figure S4 in the Supporting Information **for the GF** STM image; $a = 3.84$ nm, $b = 2.08$ nm, and $\alpha = 64°$). The ground floor of the multistory tecton patterns is clearly visible in the STM images obtained using lower biases ($|V_T| < 1000$ mV, see example of **JA1** in Figure 1 b (low bias)) and is already discernible as a less contrasted pattern at higher biases (see **JAP4**, **JA1**, **JA2**, and **JA4** in Figure 1 b,c,e (high bias), respectively), and moreover presents the same intracell organization as that of the nonfunctionalized ground floor (**GF**).[7e] Such organizations appear frozen at the single-molecule level when imaged for several hours at room temperature and at the solution–substrate interface, provided smooth tunneling parameters are applied (i.e. low current and moderate bias). This finding shows the high stability of the monolayer under ambient conditions. Moreover, although the drift prevents a given area from being observed for longer periods, a monolayer is still present with a similar domain size after leaving the sample in contact with the solution overnight. So the system has self-restoring capability, at least.

It is also highly instructive to inspect images of lattices formed using a mixture of a Janus tecton and the corresponding nonfunctionalized pedestal (Figure 1 f). It appears that Janus tectons randomly substitute nonfunctionalized pedestals in the self-assembled lattice, although at a concentration lower than in the solution. Moreover, the patterns corresponding to the pedestal of Janus tectons are then easily discernable and exactly match that of flat nonfunctionalized ones, which lie in contact with the HOPG. Therefore, the functional moiety is unambiguously identified and clearly resolved in the STM images as an additional spot specific to Janus tectons superimposed on the pedestal pattern and can only be located on top of the latter, which is exposed to the solution.

Moreover, just like their corresponding 2D tectons composed only of the base level, the Janus tectons are prochiral upon adsorption onto HOPG. As expected from such a property, two families of domains formed from adsorbates of a given enantiomer orientation are systematically observed (see Figure 1 g for an STM image of two domains with opposite symmetry). Three domain orientations that preserve the same epitaxial relationship with HOPG are possible within each such family:[8e,18] depending on the right- or left-handed character of a domain, its longer lattice axis (*b* axis) forms either a $+50.4°$ or $-50.4°$ angle with one of the three $<100>$ axes of HOPG, the other axis (*a* axis) being oriented clockwise or counterclockwise, respectively, as illustrated in Figure 1 g. In the given example, after drift correction, an angle of $\pm 51 \pm 1°$ is observed, which is in good

 © 2014 Wiley-VCH Verlag GmbH & Co. KGaA, Weinheim

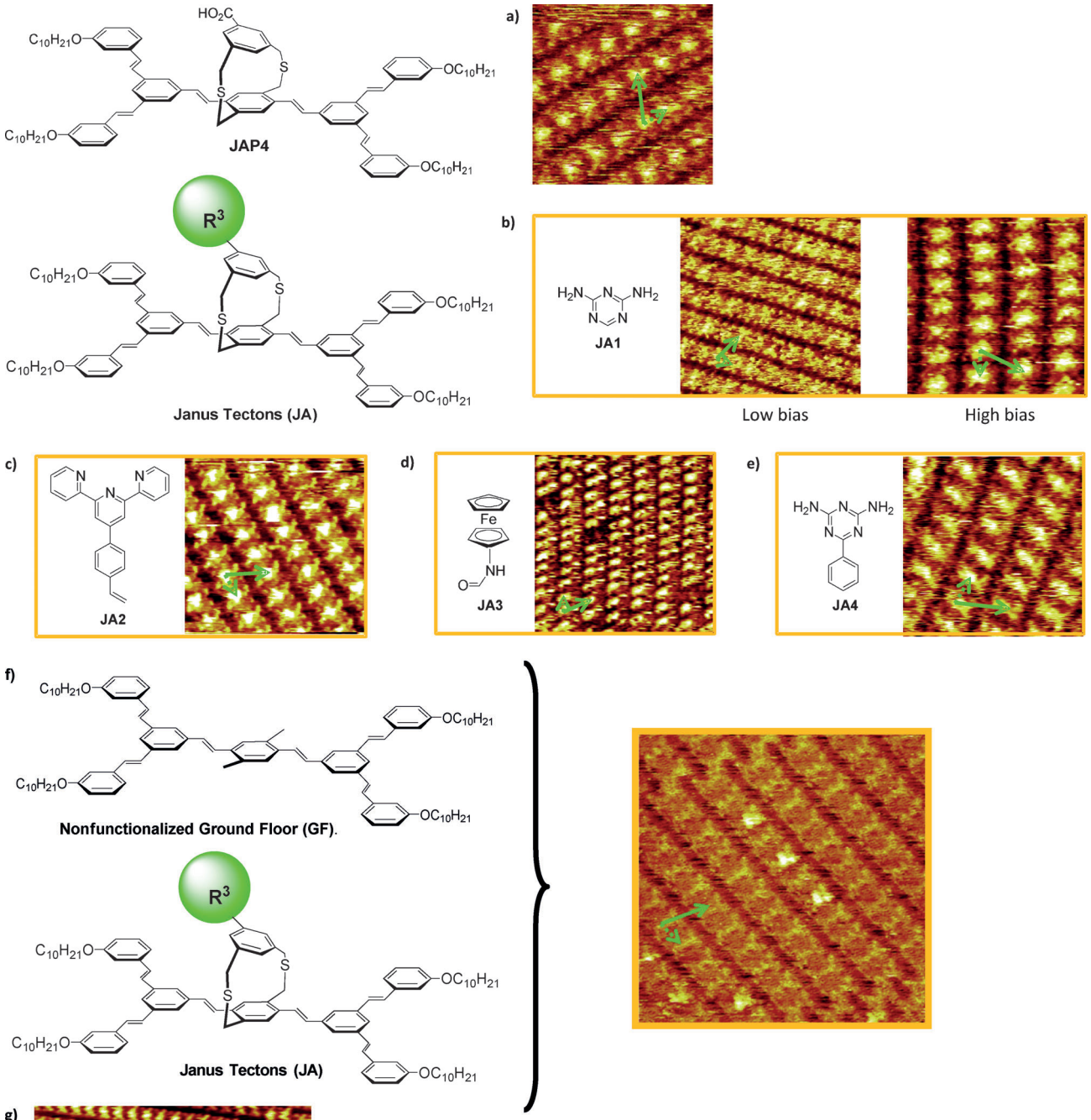

Figure 1. Self-assembly of the Janus tecton precursor (**JAP4**), all the Janus tectons (**JA1**–**JA4**), and a mixture of a Janus tecton with the nonfunctionalized ground floor (**GF**). Drift-corrected STM images obtained at the interface between HOPG and a 10^{-4} M solution in phenyloctane of a) **JAP4** (1313 nm, set point $I_T = 35$ pA, sample bias $V_B = -1200$ mV), b) **JA1** (low bias: 22×22 nm, $I_T = 8$ pA, $V_B = -950$ mV and high bias: 15×15 nm, $I_T = 14$ pA, $V_B = -1350$ mV), c) **JA2** (16×16 nm, $I_T = 25$ pA, $V_B = -1500$ mV), d) **JA3** (25×25 nm, $I_T = 20$ pA, $V_B = -1330$ mV), e) **JA4** (15×15 nm, $I_T = 40$pA, $V_B = -1380$ mV). f) A mixture of a Janus tecton with the nonfunctionalized ground floor (**GF**). Concentration ratio in the solution: ca. 1:4. One of the unit cells corresponding to the lattice formed by the nonfunctionalized pedestal ($a = 3.84$ nm, $b = 2.08$ nm, and $\alpha = 64°$) is highlighted on each image (green arrows) to illustrate the agreement between all the Janus-tecton lattices. g) Large field-of-view of a **JA3** monolayer showing two enantiomorphic domains with opposite orientations. Two mirror-symmetric 3×3 unit cells are superimposed, one on each domain. The measured angle of $\pm 51°$ between their *b*-axis and HOPG $\langle 100 \rangle$ axis is also represented.

© 2014 Wiley-VCH Verlag GmbH & Co. KGaA, Weinheim

agreement with the expected one. These observations show that both the relative positioning of the molecules inside the monolayer and also the orientation of the overall monolayer relative to the HOPG atomic lattice remain unaffected by the 3D protrusion. We can thus infer that the same process drives the self-assembly on the substrate. One explanation is that the ground level, which is either 2D in **GF** or functionalized (as in a 3D Janus tecton with whatever shape, size, or function) in **JAP** and **JA** tectons, steers the 2D self-assembly through both interactions with HOPG and with neighboring adsorbed molecules.

To confirm this image interpretation, molecular mechanics calculations were performed to model all the **JA** tecton structures and their self-assembled structures on HOPG. The upper-level bond lengths can be extracted from calculations and are between 0.91 and 1.82 nm (see Figure S5 in the Supporting Information). The calculations for related self-assembled structures permitted us to rationalize the interplay between the tectons and the graphite substrate. For every model, the structures were allowed to optimize their geometry on a fixed double layer of HOPG. This layer was a lot larger than the studied Janus tectons, and thus no preset periodic boundary conditions were used in these simulations so that the resulting theoretical structures depend only on the self-assembling properties of the molecules. Typical results for **JA2**, the tecton which has the largest group (terpyridine unit) attached to the upper level, are described (Figure 2). The parameters of the theoretical lattice for the surface-confined tecton ($a = 3.89$ nm, $b = 2.18$ nm and $\alpha = 69.8°$) determined from Figure 2b match perfectly with the experimental data extracted from the STM image of **JA2** (Figure 1c). This result demonstrates the agreement between the positioning of the Janus tectons in the optimized model and the experimental observations. The experimental and theoretical lattice values for **JA** both show that the presence of relatively large entities on the upper level does not perturb the self-assembly. Moreover these observations also show that the self-assembly is stabilized by the adsorption of alkyl chains in registry with the HOPG and by their maximized close-packing interactions through interdigitation. All these features can be partially explained by comparing the cross-sectional area of the pedestal (**GF**, $ab\sin\alpha = 7.18\ \text{nm}^2$) with the cross-sectional area occupied by each upper unit determined from calculations. As an example, in the case of **JA2** with the largest upper level (terpyridine unit), we can estimate the cross-sectional area value as around 2.02 nm^2 (see Figure S5 in the Supporting Information), which is largely compatible with the free area available around the pillar corresponding to the lattice area. More generally, it is remarkable that the clip design favors the interactions between the basis level and HOPG sufficiently to dominate the self-assembly and thus permits a fine control of the geometrical parameters for the 2D distribution of the functional unit.

Finally, the question of the self-assembly on other sp^2-carbon allotropes was addressed. The same procedure as described above was applied to monolayer graphene grown by chemical vapor deposition (CVD) onto a polycrystalline copper foil.[22] The results are reported in Figure 3. First, the atomically resolved alveolar structure of graphene was observed by STM, without application of the Janus tecton solution (Figure 3a). Then, images were acquired, at the interface between the graphene and the Janus tecton solution (Figure 3b,c). Although the imaging conditions are less stable than for HOPG, the molecular network is clearly observed through the conjugated function of the Janus tectons, with lattice parameters compatible with those obtained on graphite. Strikingly, the monolayer domains extend over rough areas and protrusions on the substrate imposed by the polycrystalline copper carrier material (as shown by Figure 3b, which was acquired over a particularly rough surface area). This shows, first, that the top-most atomic layer is able to efficiently drive the self-assembly and, second, that the graphene foil provides a long-range crystalline structural coherence that extends far beyond the carrier material defects, thus permitting well-orderd self-assembly into rather large single domains. The stability of the monolayer under ambient conditions was assessed to be similar to as on HOPG.

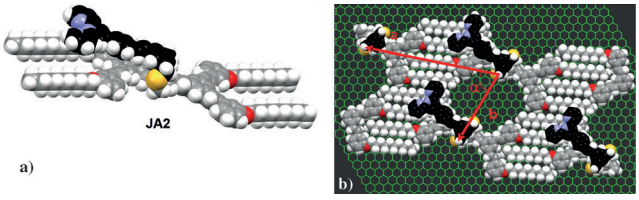

Figure 2. Theoretical description of the self-assembly of Janus tecton **JA2**. a) Schematic representation of the **JA2** structure from molecular modeling studies. b) Modeled packing of the self-assembly of **JA2** on HOPG (background green honeycomb) determined from molecular mechanics calculations (for better illustration, carbon atoms from the upper level are in black instead of gray and the calculated unit cell is shown using red arrows). The theorical unit cell ($a = 3.89$ nm, $b = 2.18$ nm, and $\alpha = 69.8°$) is shown by red arrows.

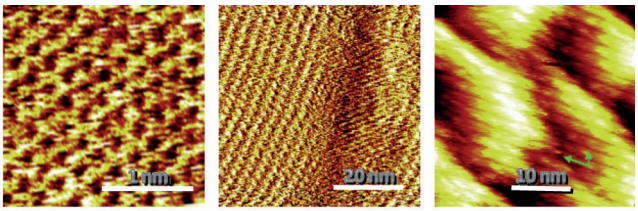

Figure 3. Self-assembly on graphene. Drift-corrected STM images obtained: a) in air on a monolayer graphene substrate grown by chemical vapor deposition on a polycrystalline copper foil showing the alveolar graphene atomic structure (2.2×2.2 nm, setpoint $I_T = 110$pA, sample bias $V_B = -350$ mV), and b,c) at the interface between this substrate and a 10^{-4} M solution of Janus tectons in phenyloctane (b: 58×58 nm, set point $I_T = 20$ pA, sample bias $V_B = -950$ mV; c: 34×34 nm, $I_T = 13$ pA, $V_B = -950$ mV). Images (a) and (b) were acquired in the current (i.e. so-called constant height) mode, whereas image (c) was acquired in the height (i.e. constant current) mode to show the substrate roughness. A unit cell corresponding to the lattice formed on HOPG ($a = 3.84$ nm, $b = 2.08$ nm, and $\alpha = 64°$) is highlighted in (c; green arrows).

© 2014 Wiley-VCH Verlag GmbH & Co. KGaA, Weinheim

In summary, for the first time a general platform for the noncovalent functionalization of flat $C(sp^2)$-based substrates including graphene has been investigated. A new general and versatile strategy based on the Janus tecton concept has been defined to obtain two library series of 3D-functionalized building blocks. We demonstrated that the self-assembled Janus tectons form, as a result of the huge cross-sectional area (footprint) of the pedestal, well-organized adlayers with a precise lateral order, with the external exposed surface presenting a wide range of functionalities ranging from chemical groups to functional units such as ligands and sandwich compounds. The reported strategy is expected to be generally applicable for generating self-assembled Janus tectons that exhibit on-demand functionalization for applications in various fields such as catalysis, electronics, photonics, and biology.

The successful self-assembly on graphene allows the fabrication of field-effect phototransistors to study the fundamental aspects of the electronic and transport properties of a graphene substrate functionalized with photoactive Janus tectons. Moreover, the long-range lateral order achieved by self-assembly on graphene provides a rational and reproducible surface functionalization, a necessary requirement for chemical sensor fabrication with good and reproducible selectivity, for example. Finally, the possibility to transfer the graphene monolayer onto various substrates considerably extends the application of our noncovalent functionalization strategy.

Received: March 21, 2014
Published online: July 22, 2014

Keywords: graphene · Janus tectons · scanning probe microscopy · self-assembly · supramolecular chemistry

[1] a) J. C. Love, L. A. Estroff, J. K. Kriebel, R. G. Nuzzo, G. M. Whitesides, *Chem. Rev.* **2005**, *105*, 1103 – 1169; b) the SAM approach is based on the chemisorption of building blocks consisting of a binding group, a spacer chain, and a functional head group. SAMs have emerged as versatile platforms for generating exposed surfaces exhibiting a wide range of well-defined functionalities (nonpolar, polar, electroactive, hydrogen bonding etc). However, functionalized SAMs offer a poor control of the lateral order and this strategy cannot be used for the functionalization of carbon allotropes such as carbon nanotubes and graphene or HOPG.

[2] J. V. Barth, G. Costantini, K. Kern, *Nature* **2005**, *437*, 671 – 679.

[3] J. V. Barth, *Annu. Rev. Phys. Chem.* **2007**, *58*, 375 – 407.

[4] L. Bartels, *Nat. Chem.* **2010**, *2*, 87 – 95.

[5] a) J. A. A. W. Elemans, S. Lei, S. De Feyter, *Angew. Chem. Int. Ed.* **2009**, *48*, 7298 – 7332; *Angew. Chem.* **2009**, *121*, 7434 – 7469; b) A. Ciesielski, C. A. Palma, M. Bonini, P. Samori, *Adv. Mater.* **2010**, *22*, 3506 – 3520; c) F. Cicoira, C. Santato, F. Rosei, *Top. Curr. Chem.* **2008**, *285*, 203 – 267; d) F. Rosei, M. Schunack, Y. Naitoh, P. Jiang, A. Gourdon, E. Laegsgaard, I. Stensgaard, C. Joachim, F. Besenbacher, *Prog. Surf. Sci.* **2003**, *71*, 95 – 146; e) Y. Yang, C. Wang, *Chem. Soc. Rev.* **2009**, *38*, 2576 – 2589; f) M. Surin, P. Samori, *Small* **2007**, *3*, 190 – 194; g) K. G. Nath, O. Ivasenko, J. A. Miwa, H. Dang, J. D. Wuest, A. Nanci, D. F. Perepichka, F. Rosei, *J. Am. Chem. Soc.* **2006**, *128*, 4212 – 4213; h) H. Zhou, H. Dang, J.-H. Yi, A. Nanci, A. Rochefort, J. D. Wuest, *J. Am. Chem. Soc.* **2007**, *129*, 13774 – 13775; i) H. Zhou, H. J. D. Wuest, *Langmuir* **2013**, *29*, 7229 – 7238.

[6] K. S. Mali, J. Adisoejoso, E. Ghijsens, I. De Cat, S. De Feyter, *Acc. Chem. Res.* **2012**, *45*, 1309 – 1320.

[7] T. Kudernac, S. Lei, J. A. A. W. Elemans, S. De Feyter, *Chem. Soc. Rev.* **2009**, *38*, 402 – 421; D. Bonifazi, S. Mohnani, A. Llanes-Pallas, *Chem. Eur. J.* **2009**, *15*, 7004 – 7025.

[8] a) D. Kühne, F. Klappenberger, R. Decker, U. Schlickum, H. Brune, S. Klyatskaya, M. Ruben, J. V. Barth, *J. Am. Chem. Soc.* **2009**, *131*, 3881 – 3883; b) G. Schull, L. Douillard, C. Fiorini-Debuisschert, F. Charra, F. Mathevet, D. Kreher, A.-J. Attias, *Nano Lett.* **2006**, *6*, 1360 – 1363; c) G. Schull, L. Douillard, C. Fiorini-Debuisschert, F. Charra, F. Mathevet, D. Kreher, A.-J. Attias, *Adv. Mater.* **2006**, *18*, 2954 – 2957; d) S. Furukawa, K. Tahara, F. C. De Schryver, M. Van der Auweraer, Y. Tobe, S. De Feyter, *Angew. Chem. Int. Ed.* **2007**, *46*, 2831 – 2834; *Angew. Chem.* **2007**, *119*, 2889 – 2892; e) D. Bléger, D. Kreher, F. Mathevet, A. J. Attias, G. Schull, A. Huard, L. Douillard, C. Fiorini-Debuischert, F. Charra, *Angew. Chem. Int. Ed.* **2007**, *46*, 7404 – 7407; *Angew. Chem.* **2007**, *119*, 7548 – 7551; f) J. Adisoejoso, K. Tahara, S. Okuhata, S. Lei, Y. Tobe, S. De Feyter, *Angew. Chem. Int. Ed.* **2009**, *48*, 7353 – 7357; *Angew. Chem.* **2009**, *121*, 7489 – 7493.

[9] M. Koepf, F. Chérioux, J. A. Wytko, J. Weiss, *Coord. Chem. Rev.* **2012**, *256*, 2872 – 2892.

[10] a) M. D. Watson, F. Jäckel, N. Severin, J. P. Rabe, K. Müllen, *J. Am. Chem. Soc.* **2004**, *126*, 1402 – 1407; b) F. Matino, G. Schull, F. Köhler, S. Gabutti, M. Mayor, R. Berndt, *Proc. Natl. Acad. Sci. USA* **2011**, *108*, 961 – 964.

[11] a) H. Tanaka, T. Ikeda, M. Takeuchi, K. Sada, S. Shinkai, T. Kawai, *ACS Nano* **2011**, *5*, 9575 – 9582; b) J. Otsuki, Y. Komatsu, D. Kobayashi, M. Asakawa, K. Miyake, *J. Am. Chem. Soc.* **2010**, *132*, 6870 – 6871; c) D. Écija, W. Auwärter, S. Vijayaraghavan, K. Seufert, F. Bischoff, K. Tashiro, J. V. Barth, *Angew. Chem. Int. Ed.* **2011**, *50*, 3872 – 3877; *Angew. Chem.* **2011**, *123*, 3958 – 3963.

[12] B. Baisch, D. Raffa, U. Jung, O. M. Magnussen, C. Nicolas, J. Lacour, J. Kubitschke, R. Herges, *J. Am. Chem. Soc.* **2009**, *131*, 442 – 443; b) S. Venkataramani, U. Jana, M. Dommaschk, F. D. Sönnichsen, F. Tuczek, R. Herges, *Science* **2011**, *331*, 445 – 4483.

[13] Alternative bottom-up approaches to achieve periodical 3D order on the surface have been reported in the literature, for example, well-controlled epitaxial growth of stable bulk functional materials with a 3D lattice that permits accurate structural ordering, as illustrated with 3D metal – organic frameworks (MOFs). For example, see O. Shekhah, H. Wang, M. Paradinas, C. Ocal, B. Schüpbach, A. Terfort, D. Zacher, R. A. Fischer, C. Wöll, *Nat. Mater.* **2009**, *8*, 481 – 484.

[14] a) V. Georgakilas, M. Otyepka, A. B. Bourlinos, V. Chandra, N. Kim, K. C. Kemp, P. Hobza, R. Zboril, K. S. Kim, *Chem. Rev.* **2012**, *112*, 6156 – 6214; b) X.-Y. Fan, R. Nouchi, L.-C. Yin, K. Tanigaki, *Nanotechnology* **2010**, *21*, 475208; c) P. Järvinen, S. K. Hämäläinen, K. Banerjee, P. Häkkinen, M. Ijäs, A. Harju, P. Liljeroth, *Nano Lett.* **2013**, *13*, 3199 – 3204.

[15] a) M. Urdampilleta, S. Klyatskaya, J.-P. Cleuziou, M. Ruben, W. Wernsdorfer, *Nat. Mater.* **2011**, *10*, 502 – 506; b) J. A. Mann, J. Rodriguez-Lopez, H. D. Abruna, W. R. Dichtel, *J. Am. Chem. Soc.* **2011**, *133*, 17614 – 17617; c) S. Qu, M. Li, L. Xie, X. Huang, J. Yang, N. Wag, S. Yang, *ACS Nano* **2013**, *7*, 4070 – 4081.

[16] a) Q. H. Wang, M. C. Hersam, *Nat. Chem.* **2009**, *1*, 206 – 211; b) Q. H. Wang, M. C. Hersam, *Nano Lett.* **2011**, *11*, 589 – 593.

[17] a) J. M. MacLeod, F. Rosei, *Small* **2014**, *10*, 1038 – 1049.

[18] D. Bléger, F. Mathevet, D. Kreher, A. J. Attias, A. Bocheux, S. Latil, L. Douillard, C. Fiorini-Debuisschert, F. Charra, *Angew. Chem. Int. Ed.* **2011**, *50*, 6562 – 6566; *Angew. Chem.* **2011**, *123*, 6692 – 6696.

 © 2014 Wiley-VCH Verlag GmbH & Co. KGaA, Weinheim

[19] a) D. Bléger, Thesis Université Paris 6, **2008**; b) R. Annunziata, M. Benaglia, F. Cozzi, A. Mazzanti, *Chem. Eur. J.* **2009**, *15*, 4373 – 4381; c) J. L. Xia, S. H. Liu, F. Cozzi, M. Mancinelli, A. Mazzanti, *Chem. Eur. J.* **2012**, *18*, 3611 – 3620; d) X. Zhu, Y. Ou, J. Zhang, J. L. Xia, J. Yin, G. A. Yu, S. H. Liu, *Dalton Trans.* **2013**, *42*, 7177 – 7189; e) J. Xia, Y. P. Ou, X. G. Meng, J. Yin, G. A. Yu, S. H. Liu, *Eur. J. Inorg. Chem.* **2014**, 247 – 255.

[20] M. Wolffs, S. J. George, Ž. Tomović, S. C. J. Meskers, A. P. H. J. Schenning, E. W. Meijer, *Angew. Chem. Int. Ed.* **2007**, *46*, 8203 – 8205; *Angew. Chem.* **2007**, *119*, 8351 – 8353.

[21] A. Winter, D. A. M. Egbe, U. S. Schubert, *Org. Lett.* **2007**, *9*, 2345 – 2348.

[22] Z. Han, A. Kimouche, A. Allain, H. Arjmandi-Tash, A. Reserbat-Plantey, S. Pairis, V. Reita, N. Bendiab, J. Coraux, V. Bouchiat, *Adv. Funct. Mater.* **2014**, *24*, 964 – 970.

 © 2014 Wiley-VCH Verlag GmbH & Co. KGaA, Weinheim